Functional characterization of GNAS mutations found in patients with pseudohypoparathyroidism type Ic defines a new subgroup ofpseudohypoparathyroidism affecting selectively Gsα-receptor interaction.

Published in final edited form as:
Hum Mutat. 2011 June ; 32(6): 653–660. doi:10.1002/humu.21489.

Functional characterization of *GNAS* mutations found in patients with pseudohypoparathyroidism type Ic defines a new subgroup of pseudohypoparathyroidism affecting selectively Gsα-receptor interaction

Susanne Thiele[1], **Luisa de Sanctis**[2], **Ralf Werner**[1], **Joachim Grötzinger**[4], **Cumhur Aydin**[3,5], **Harald Jüppner**[3], **Murat Bastepe**[3], and **Olaf Hiort**[1]

[1]Department of Pediatrics and Adolescent Medicine, University of Lübeck, Germany

[2]Department of Pediatrics, University of Turin, Italy

[3]Endocrine Unit, Massachusetts General Hospital and Harvard Medical School, Boston, USA

[4]Institute of Biochemistry, Christian-Albrechts-University of Kiel, Germany

[5]Department of Endodontics, Center for Dental Sciences, Gülhane School of Medicine, Ankara, Turkey

Abstract

Pseudohypoparathyroidism type Ia (PHPIa) is caused by *GNAS* mutations leading to deficiency of the α-subunit of stimulatory G proteins (Gsα) that mediate signal transduction of G protein-coupled receptors via cAMP. PHP type Ic (PHPIc) and PHPIa share clinical features of Albright hereditary osteodystrophy (AHO); however, *in vitro* activity of solubilized Gsα protein is normal in PHPIc but reduced in PHPIa. We screened 32 patients classified as PHPIc for *GNAS* mutations and identified three mutations (p.E392K, p.E392X, p.L388R) in four unrelated families. These and one novel mutation associated with PHPIa (p.L388P) were introduced into a pcDNA3.1(−) expression vector encoding Gsα wild-type and expressed in a Gsα-null cell line (Gnas $^{E2-/E2-}$). To investigate receptor-mediated cAMP accumulation, we stimulated the endogenous expressed β_2-adrenergic receptor, or the co-expressed PTH- or TSH receptors, and measured the synthesized cAMP by RIA. The results were compared to receptor-independent cholera toxin-induced cAMP accumulation. Each of the mutants associated with PHPIc significantly reduced or completely disrupted receptor-mediated activation, but displayed normal receptor-independent activation. In contrast, PHPIa associated p.L388P disrupted both receptor-mediated activation and receptor-independent activation. We present a new subgroup of PHP that is caused by Gsα deficiency and selectively affects receptor-coupling functions of Gsα.

Keywords

Pseudohypoparathyroidism; PHP; Albright hereditary osteodystrophy; Gsα; GNAS

Address all correspondence and requests for reprints to: Susanne Thiele, MD, Division of Pediatric Endocrinology and Diabetes, Department of Pediatrics and Adolescent Medicine, University of Lübeck, Ratzeburger Allee 160, 23538 Lübeck, Germany, Fon: +49-451-500-2191, Fax: +49-451-500-6867, thiele@paedia.ukl.mu-luebeck.de.

Disclosure Statement: The authors have nothing to disclose.

Introduction

The term pseudohypoparathyroidism (PHP) describes a group of related rare disorders characterized by end organ-resistance to PTH and other peptide hormones that mediate their actions through G protein-coupled receptors (GPCRs) via cAMP/ protein kinase A. Based on clinical and laboratory findings, and on the result of Gsα protein activity *in vitro*, PHP has been divided into different subgroups. PHP type Ia (PHPIa; MIM# 103580) is commonly caused by heterozygous, maternally inherited inactivating mutations involving those exons of the *GNAS* locus (MIM# 610540) that encode the α-subunit of the stimulatory G protein (Gsα). These mutations lead to Gsα deficiency. Because there are some imprinted tissues where this signaling protein is derived only or predominantly from the maternal allele, including proximal renal tubules, thyroid, ovaries, and pituitary, affected individuals develop PTH-resistance leading to hypocalcemia and hyperphosphatemia, as well as resistance towards TSH and, sometimes, other peptide hormones and ligands. Due to haploinsufficiency of Gsα in non-imprinted tissues, patients affected by PHPIa develop additional features of Albright hereditary osteodystrophy (AHO), which include round face, short stature, brachymetacarpia, ectopic ossification, and mental retardation. Patients also sometimes present with obesity.

Paternally inherited *GNAS* mutations lead to pseudo-PHP (PPHP; MIM# 612463) characterized by some features of AHO in the absence of hormone resistance (reviewed in Weinstein et al., 2002; Bastepe and Jüppner, 2005; Bastepe, 2008). Both, PHPIa and PPHP, show diminished Gsα protein activity as determined by an *in vitro* assay using solubilized Gsα from readily accessible cells such as red blood cells or fibroblasts and non-hydrolyzable guanosine 5'-[γ-thio]triphosphate (GTPγs) (Levine et al., 1980, 1988). Gsα protein activity measurement has often been decribed as the first diagnostic step, followed by a molecular genetic analysis of *GNAS*.

PHP type Ib (PHPIb; MIM# 603233) is associated with the loss of methylation at one or more maternally methylated regions within *GNAS* and can be caused by heterozygous, maternally inherited deletions up-stream of or within the *GNAS* locus or can occur sporadically (Jüppner et al., 1998, 2006; Bastepe et al., 2001). As a result, Gsα expression is reduced in a few tissues including the renal proximal tubules and, in some cases, the thyroid, leading to PTH-resistant hypocalcemia and hyperphosphatemia and occasionally elevated TSH levels. Typically, PHPIb patients lack AHO features and present with normal Gsα activity (Bastepe, 2008). Recently, patients with PHP and AHO features have been described in association with methylation changes of *GNAS* (de Nanclares et al., 2007; Mantovani et al., 2010), which are not included in the current classification of the disorders.

Pseudohypoparathyroidism type Ic (PHPIc; MIM# 612462) describes individuals who develop the same clinical and laboratory abnormalities as patients with PHPIa, including AHO and peptide hormone resistance, but in contrast to PHPIa, *in vitro* assessment of Gsα protein activity reveals no abnormality (Table 1) (Weinstein, 1998). It has therefore been postulated that PHPIc may not be caused by a functional impairment of the Gsα protein, but by another component of the cAMP-dependent signaling pathway, such as adenylyl cyclase, inhibitory G proteins, or phosphodiesterases (Farfel et al., 1981; Lania et al., 2001; Aldred, 2006; Mantovani and Spada, 2006).

We screened a cohort of patients classified as PHPIc (based on clinical and laboratory data and the result of the *in vitro* assay) and found mutations in the *GNAS* gene in a subgroup. We then performed functional analysis of three naturally occurring mutations located in the extreme C-terminus of Gsα. By analyzing the receptor-mediated activation of the Gsα-mutants in a mouse Gsα-null fibroblast-like cell line (Gnas $^{E2-/E2-}$) and comparing the

results to receptor-independent activation, we demonstrate that these mutations selectively affect receptor-coupling but not adenylyl cyclase activating functions of Gsα, while the PHPIa associated mutation affects both.

Patients and methods

We screened 32 patients with PHP, AHO and normal measured Gsα protein activity for mutations in exons 1–13 of *GNAS* including exon/intron boundaries. Here, we only describe the phenotype and history of patients in whom we found *GNAS* mutations. The clinical and laboratory data are summarized in Table 2

Patient A

The male patient was delivered at term after an uneventful pregnancy by Caesarian section. During birth he suffered from asphyxia, which was initially thought to be the cause of a delay of his speech and psychomotoric development. At the age of 12 years, he was hospitalized because of facial nerve palsy. He showed characteristic AHO features, including round face, shortening of the 4^{th} and 5^{th} metacarpals and mental retardation with an IQ of 40 (assessed by HAWIK). His mother had only mild signs of AHO, including short stature (154 cm, $<3^{rd}$ centile), and brachymetacarpia of the 4^{th} metacarpals, but no other AHO features, and no evidence for hormonal resistance, consistent with the diagnosis of PPHP. The patient does not have siblings and the father is healthy.

Patient B

The female patient was born at term after an uneventful pregnancy as the only child of their parents. AHO and PHP were diagnosed at the age of 5.5 years when she presented at the endocrine clinic with round face, brachymetacarpia of the 3^{rd}, 4^{th}, and 5^{th} metacarpals and obesity (22.5 kg, BMI 19.6 kg/ m^2, $>97^{th}$ centile). Her mother presented with brachymetacarpia but no other AHO features and PTH and TSH levels were in the normal range, consistent with the diagnosis of PPHP. The father did not present any AHO signs.

Patient C

The patient is a female, born at 38 weeks of gestation as the only child of their parents. Diagnosis of AHO and PHP was suspected because of neonatal hypothyroidism. At 11 months of age she had a round face, her length was 65.5 cm ($<3^{rd}$ centile), she had already developed brachymetacarpia affecting the 4^{th} and 5^{th} phalanges and her weight was 7.8 kg (BMI 18,4 kg/m^2, 90^{th} centile). Her mother was of short stature (142 cm, $<3^{rd}$ centile) and had also brachymetacarpia, but no hormonal resistances.

Patient D1

The patient is a male twin born at term. He came for endocrinological assessment at the age of 13 years because of recurrent hypocalcemia, and presented with round face and brachymetacarpia of the 4^{th} and 5^{th} phalanges.

Patient D2

The patient is the twin sister of D1 with an uneventful medical history until the age of 13 years. At this time, her weight was slightly elevated (55 kg, BMI 26.5 kg/m^2, 97^{th} centile) and she presented with round face and brachymetacarpia. The mother of both children had a round face, was of short stature (152 cm, $<3^{rd}$ percentile), and demonstrated brachymetacarpia of the 4^{th} and 5^{th} metacarpals and metatarsals, but no hormonal alterations or further AHO signs. The father of both children is healthy.

Patient E

The female patient was born after uneventful pregnancy. She was hospitalized at the age of 4 years when she presented with hypocalcemic seizures. At this time she demonstrated a round face, brachymetacarpia of the 5th metacarpals, and obesity (20.7 kg, >97th centile), but no other signs of AHO. Her mother also presented with short 5th metacarpals, however, PTH and TSH levels were in the normal range. The patient does not have siblings and the father does not show abnormalities.

Patients B, D1 and D2 have in part already been described by de Sanctis (de Sanctis et al., 2003). Laboratory investigations at the time of diagnosis revealed for all patients elevated PTH and TSH levels. Vitamin D deficiency had been excluded before by measuring 25-OH-vitamin D levels within the reference range. The *in vitro* Gsα activity was normal, except for patient E, (activity was reduced to 71%), when compared to healthy controls. All subjects or their guardians gave informed consent to the study. Studies were approved by the ethical committee of the University of Lübeck as part of the funded project on AHO (see acknowledgment).

Gsα protein activity and mutation analysis—The activity of Gsα protein from erythrocyte membranes of patients was investigated in heparinized blood samples as described earlier (Levine et al., 1980; Ahrens et al., 2001). Briefly, after solubilization the Gsα protein from patient derived erythrocyte membranes was incubated with GTPγS. We added adenylyl cyclase from turkey red cell membranes and measured the generated cAMP in the presence of ATP by RIA (Immuno Biological Laboratories, Hamburg, Germany). Results obtained in triplicate were expressed as percent of the mean of healthy controls (normal range: 85–115 %). For molecular genetic analysis we isolated genomic DNA derived from peripheral leukocytes by standard procedures (Qiaquick DNA kit, Qiagen, Hilden, Germany). *GNAS* exon 1–13, (RefSeq NM_000516.4) including all intron/exon boundaries were amplified in 11 fragments by PCR (primer sequences available upon request). PCR-amplified DNA was sequenced by direct cycle sequencing using the BigDye Terminator v1.1 Cycle Sequencing Kit (Applied Biosystems, Foster City, CA) and an ABI 3130 capillary sequencer (Applied Biosystems, Foster City, CA).

Site-directed mutagenesis of expression plasmids—We introduced the detected mutations p.E392K, p.E392X, p.L388R and p.L388P into a pcDNA3.1(−) vector encoding wild-type rat Gsα (which is identical to human Gsα), in which a shortened hemagglutinine epitope-tag (DVPDYA) had been introduced into exon 3 by PCR-based mutagenesis (Bastepe et al., 2002). The first PCR amplification was carried out by using a sense primer in exon 4 and an antisense primer comprising the respective mutation. A second PCR was performed using a sense primer containing the mutation and an antisense primer (Bghas) located downstream of Gsα. PCR products were used as a template in a third PCR using the exon 4-sense and the Bgh-antisense primer. PCR products were amplified in a Mastercycler Gradient (Eppendorf, Hamburg, Germany) using the following cycling protocol: denaturation for 30 s at 98 C, followed by 29 cycles denaturation (10 s at 98 C), annealing (30 s at 64 C), and elongation (45 s at 72 C) and 1 final cycle (10 min at 72 C). The reaction mix contained 100 ng vector DNA, 1x Phusion-buffer HF, 2.5 U Phusion High-Fidelity DNA-Polymerase (New England Biolabs) and 200 μM dNTPs (Fermentas, St. Leon-Rot, Germany). The amplicon including the respective mutation was double digested with *Afe*I and *Hin*dIII (New England Biolabs, Beverley, CA) and subcloned into the original Gsα expression vector. All clones were verified by nucleotide sequence analysis including the entire inserts up to cloning borders.

Cell culture, transfection, and stimulation—For transfection experiments, we used $Gnas^{E2-/E2-}$ cells, a clonal murine cell line in which *Gnas* exon 2 had been disrupted and thus does not express endogenous Gsα or XLαs (Bastepe et al., 2002). Cells were seeded into 24-well plates at a density of 60–80 %. After 24 h, the cells were transfected with 0.2 μg/well of plasmid DNA encoding Gsα using Effectene (Qiagen, Valencia, CA). For cotransfection experiments with plasmids encoding the human TSH receptor (TSHR) or the human PTH receptor (PTHR), the total amount of DNA per well was 0.4 μg, which was kept constant by addition of empty vector. Cells were cultured at 37 C for 72 h with daily exchanges of DMEM-F12-medium containing 10 % fetal bovine serum followed by stimulation with different agonists. For determination of cholera toxin (CTX)-induced cAMP formation, cells were treated at 37 C for 2 h with 1 μg/ml CTX (Sigma-Aldrich Corp., St. Louis, MO). Stimulation with Isoproterenol (Iso; Sigma-Aldrich Corp., St. Louis, MO), human $[Y^{34}]$PTH(1–34)amide (hPTH) (Massachusetts General Hospital, Biopolymer Core Facility, Boston, USA) and human TSH (Sigma-Aldrich Corp., St. Louis, MO) were carried out in the presence of F12-DMEM containing HEPES-NaOH, 1 mg/ml BSA, and 2 mM isobutylmethylxanthine (Sigma-Aldrich Corp., St. Louis, MO). Treatment was followed by 15 min incubation at 37 C in a water bath. After incubation cells were lysed by 50 nM HCl and cAMP accumulation in each well was determined by RIA as previously described (Bastepe et al., 2002). All transfection experiments in this study were repeated at least three times.

Western blot analysis—For Western blot analysis, 15 μg of cellular protein were loaded onto a 12 % polyacrylamide gel. Electrophoresis was carried out at 100 V for 120 min in a Mini-Protean 3 chamber (BioRad, Munich, Germany). Proteins were transferred to nitrocellulose membranes (BA85, Schleicher & Schüll, Dassel, Germany) at 100 V for 80 min using a Mini Trans-Blot cell (BioRad, Munich, Germany) and using a blotting buffer containing 16.5 mM Tris, 150 mM glycine and 20 % (V/V) methanol. Non-specific binding sites were blocked by immersing the membranes overnight at 4 C in 5% non-fat milk (Becton-Dickinson, Franklin Lakes, USA) dissolved in PBS/ Tween buffer (containing 137 mM NaCl, 2.7 mM KCl, 10 mM Na_2HPO_4, 2 mM KH_2PO_4, 0.1 % Tween 20, pH 7.4). The blocked membranes were incubated with an HA-antibody (Y11: sc805, Santa Cruz Biotechnology) diluted 1:100 in blocking buffer for 1 h at room temperature. The membrane was rinsed 4 times for 15 min in PBS/Tween buffer and incubated with an anti-rabbit IgG peroxidase conjugate at a dilution of 1:1000 (Sigma, Taufkirchen, Germany) for 1 h. After rinsing the membrane as above, protein bands were visualized using the Western Lightning Chemiluminescence Reagent Plus substrate (Perkin Elmer, Boston, MA) and the Fusion SL detection system (Vilber Lourmat, Eberhardzell, Germany).

Statistical analysis and structural analysis—Student´s *t* test for two independent samples was used to determine significance of observed differences of the cAMP levels after CTX-mediated stimulation of Gsα-388R (corresponding to the p.L388R mutant of Gsα) and Gsα-388P and after Isoproterenol-mediated stimulation of Gsα-392K and Gsα-392X. GraphPad 4.0 was used for determination of the EC_{50}. For the structural analysis the crystal structure of Gsα in complex with GTPγ-s (Sunahara et al., 1997) has been used. The structural representations were generated using the RIBBONS software (Kraulis, 1991).

Results

In 5 patients with PHPIc from 4 unrelated families our analysis of *GNAS* (RefSeq NM_000516.4) revealed 3 different heterozygous mutations in exon 13 affecting the two residues 388 and 392 in the carboxy-terminal portion of Gsα. In addition, we found one further mutation also affecting the residue 388, but associated with PHPIa.

In patient A and his mother, a single nucleotide exchange in codon 388 (c.1163T>G) was identified, leading to an arginine instead of a leucine (p.L388R). This mutation has not been described so far. A missense mutation in codon 392 (c.1174G>A) was identified in patient C and her mother, resulting in a substitution of glutamic acid by lysine (p.E392K). In patient B, D1, and D2 and their mothers we confirmed the heterozygous nucleotide change (c. 1174G>T) at codon 392 in concordance to the previously results in these patients (de Sanctis et al., 2003) resulting in a stop codon (p.E392X). In patient E and her mother (PHPIa), we also found a novel heterozygous change at codon 388 (c.1163T>C) resulting in proline instead of a leucine (p.L388P). Nucleotide numbering reflects cDNA numbering system with corresponding to the A of the ATG translation initiation codon in the reference sequence (NM_000516.4), according to the journal guidelines (www.hgvs.org/mutnomen).

The analysis of the remaining 27 patients with PHPIc did not reveal mutations in the Gsα encoding region of *GNAS*. All variants were not detected in 100 normal individuals and all involve highly conserved amino acids (Table 3). The mutations are summarized in Table 2. The mutations were included in the Leiden Open Variation Database (http://www.lovd.nl/GNAS) according to the nomenclature of the HGVS site. In this report, however, the commonly used nomenclature of Kosaza et al. (1988) has been used.

First we studied the ability of the missense mutants Gsα-388R and Gsα-392K (corresponding to p.L388R and p.E392K encoded in the Gsα-encoding vector) to be stimulated by the β_2-adrenergic receptor expressed endogenously in our $Gnas^{E2-/E2-}$ fibroblast-like cells. Receptor mediated cAMP accumulation in response to 10^{-5}M Isoproterenol was measured after transient expression of mutant or wild-type Gsα. The results were compared to CTX-induced cAMP accumulation, which stimulates adenylyl cyclase by ADP-ribosylation independent of receptor activation (CTX-stimulated wild-type Gsα was set as maximal stimulation of 100%).

After Isoproterenol stimulation Gsα-388R failed to induce any increase in intracellular cAMP (mean 4.5 %, SEM ±0.3), compared to the basal cAMP level (mean 3.6 % of max, SEM ±1.1), despite nearly normal CTX-induced cAMP levels (mean 81.1 % of max, SEM ±8.2). In contrast, Gsα-392K was activated by Isoproterenol, but maximal cAMP levels were only about 50% of wild-type (mean 43.6% of max, SEM ±3), whereas the CTX-induced cAMP accumulation was comparable to that of the wild-type (mean 105.6 %, SEM ±8.3) (Figure 1a). Non-transfected cells or cells transfected with the empty pcDNA3.1(−) vector, which were used as negative controls, failed to show an increase in basal, CTX- and Isoproterenol-stimulated cAMP levels (data not shown).

To determine whether cAMP accumulation of the wild-type and the mutants is dependent on agonist levels, we stimulated the cells with concentrations of Isoproterenol ranging from 10^{-4} to 10^{-8} M. Isoproterenol treatment increased cAMP formation in a dose-dependent manner in cells transiently expressing the wild-type Gsα ($EC_{50}=10^{-5.895}$ M; 95 % confidence interval $10^{-5.979}$ to $10^{-5.811}$). Consistent with our previous experiments, Isoproterenol failed completely to increase cAMP generation in cells transiently expressing Gsα-388R (mean 5.8 %, SEM ±0.2). Gsα-392K led to a significant increase in cAMP formation in response to agonist treatment with EC_{50} values ($EC_{50}=10^{-5.995}$ M; 95 % confidence interval $10^{-6.108}$ to $10^{-5.883}$) similar to wild type Gsα; however, maximal response after stimulation with 10^{-4} M was reduced to about 50 % (mean 49.8 %, SEM ±4.4) (Figure 1b).

Since all patients presented with PTH resistance, experiments with cells transiently expressing both Gsα-mutants/wild-type and the PTHR were performed. Stimulation with 10^{-8} M PTH revealed a similar pattern for Gsα-388R and Gsα-392K to that observed after

stimulation of the endogenous β_2-receptor. Gsα-388R did not show any response after agonist stimulation (mean 16.73 % of max, SEM ±0.33) and Gsα-392K led to a diminished response to about 60 % (mean 60.5 % of max, SEM ±1.86) compared to the wild-type (mean 100 %, SEM ±3.31). These results were confirmed by dose dependent agonist stimulation (Figure 1c). The EC_{50} for PTH-induced cAMP accumulation through Gsα-392K ($10^{-9.307}$ M) was similar as for wild-type Gsα ($10^{-9.102}$ M).

Furthermore, we cotransfected cDNA encoding the human TSHR and the vectors containing the Gsα-mutants, and stimulated the cells with 10 mIU/ml TSH. Again, the Gsα-388R mutant was unable to transduce receptor-mediated cAMP response, and Gsα-392K led to a diminished response. Transfection with the empty vector, or the TSHR alone used as negative controls did not elevate the cAMP levels after stimulation with TSH (results not shown).

To investigate whether our cell model can discriminate different functional effects of mutations leading to the PHPIa or the PHPIc-subtype even if located in the same residue, we transfected the $Gnas^{E2-/E2-}$ cells with Gsα-388P associated with PHPIa. We compared the results to those of Gsα-388R. As Gsα-388R (mean 4.2 %, SEM ±1.2), Gsα-388P could not be stimulated by Isoproterenol (mean 3.4 %, SEM ±1). However, in concordance to the reduced Gsα protein activity in erythrocyte membranes leading to the diagnosis of PHPIa in this patient, the CTX-induced stimulation by Gsα-388P was reduced to nearly 60 % (mean 55.98 % of max, SEM ±2.95), compared to the wild-type (mean 100 %, SEM ±3.9). In contrast, the CTX-induced stimulation of Gsα-388R was similar to the wild type (mean 92.48 %, SEM ±7) (Figure 2a).

We also investigated the nonsense mutation Gsα-392X found in our patients B, D1 and D2 and compared the results to those of the missense mutant Gsα-392K affecting the same residue. In contrast to our findings in Gsα-392K (32.19 % of max, SEM ±0.14), we could not demonstrate any significant stimulation via the β_2-receptor in Gsα-392X (mean 7.32 % of max, SEM ±0.36) (Figure 2b).

The CTX-induced cAMP accumulation of the PHPIc associated mutants Gsα-388R, Gsα-392K, and Gsα-392X did not show significant differences to the wild-type, but the PHPIa associated mutant Gsα-388P led to diminished CTX-induced cAMP synthesis. To rule out different expression levels between Gsα-388P and the wild-type Gsα, we established immunoblot analysis using hemagglutinine-tag specific antibody and demonstrated equivalent expression of all mutants except a slightly reduced expression of Gsα-392X (Figure 2c).

Discussion

Historically, the term PHPIc has been used for a constellation including PHP, AHO signs and a normal Gsα activity measured *in vitro*. Therefore, PHPIc is thought to be caused by impairment of another component of the cAMP-dependent pathway than Gsα (Aldred, 2006; Mantovani and Spada, 2006). In our study we demonstrate in a subset of patients with the former diagnosis PHPIc inherited maternal inactivating mutations in the Gsα encoding exons of *GNAS*. Furthermore, we prove impaired interaction between different GPCRs and the mutated Gsα forms leading to deficient Gsα signalling. Since these mutations lead, in contrast to classical PHPIc, to Gsα deficiency and affect, in contrast to PHPIa, selectively Gsα-receptor coupling functions, this constitutes a new subgroup of PHP based on distinct molecular dysfunction of Gsα.

Two further patients harboring *GNAS* mutations with similar functional deficits have been described. The nonsense mutation p.Y391X was identified in a PHPIc patient (Linglart et

al., 2002) and molecular investigation of this Gsα-mutant led to the proposal that PHPIc represents a subgroup of PHPIa in which the *GNAS* mutations affect receptor-coupling (Linglart et al., 2006; Bastepe, 2008). The second described patient (harboring the mutation p.R385H) also demonstrated impaired receptor-coupling without disturbing downstream Gsα signaling. However, since the assay used for diagnosis did involve GPCR-Gsα coupling the patient was termed as having PHPIa (Schwindinger et al, 1994).

All *GNAS* mutations found in our patients are located in the α5-helix concerning the extreme carboxyl-terminus of Gsα (which is highly conserved between different species, see Table 3), whereas usually PHPIa-associated mutations are distributed throughout the gene (www.hgmd.cf.ac.uk). The results from a variety of studies implicate that this region contains the major sites for interaction between Gsα and GPCRs (Sullivan et al., 1987; Masters et al., 1988; Spiegel et al., 1990; Pantoloni et al., 1993; Rasenick et al., 1994; Hamm et al., 1998; Linglart et al., 2006; Zang et al., 2006). Consistent with these results, our data demonstrate that natural mutations located at the carboxy-terminal end of Gsα can disrupt or strongly impair the ability for receptor-coupling despite normal CTX- or GTPγs induced adenylyl cyclase activity.

The Gsα-388R-mutant showed a complete loss of receptor-mediated stimulation of the β_2-adrenergic receptor, the PTHR, and the TSHR, indicating a crucial role of this residue for receptor-coupling. We analyzed the three dimensional structure of *GNAS* that has been described previously (Sunahara et al., 1997) to examine the putative effects of the mutation (Figure 3). The hydrophobic side chain of L388 of the α5-helix is part of the accessible surface of the molecule and thus directly involved in contact of Gsα to the GPCR. The p.L388R will introduce a positive charge at this position and thus interfere with receptor binding.

The mutation p.L388P, associated with PHPIa, also leads to a reduced response to receptor-independent activation. Normally, the backbone amide group of L388 forms a hydrogen bond with the carbonyl group of Q384. Since proline is, in contrast to arginine, not able to form such a helix stabilizing hydrogen bond, the p.L388P mutation will lead to destabilization of the α5-helix and thereby may disturb the whole tertiary structure of the molecule and thus reduce not only the receptor-dependent, but also the receptor-independent stimulation.

The missense mutant Gsα-392K demonstrated a residual activity after receptor-coupled stimulation with Isoproterenol, while in contrast the nonsense mutant Gsα-392X led to a complete loss of receptor-mediated activation through β_2-receptor stimulation. These results seem to be reflected even by the severity of PTH and TSH resistance found in the patients (see Table 2). This strongly suggests that the last three amino acid residues of Gsα are essential for receptor-coupling and the results are in agreement with the findings of Linglart, who demonstrated a complete loss of the β_2-adrenergic receptor-mediated activation by the p.Y391X-mutant that lacks the last four residues of Gsα (Linglart et al., 2006). In addition, the loss of the last three amino acids may lead to instability of the protein, as suggested by slightly reduced expression of Gsα-392X in our Western blotting analysis (Figure 2c).

Although, we identified *GNAS* mutations in a subset of designated PHPIc patients, the ethiopathogenesis of the remaining 27 cases remains to be elucidated. In the literature, two PHPIc patients have been described in whom the disease is caused by epigenetic changes involving the *GNAS* locus (de Nanclares et al., 2007). However, several patients with the diagnosis of PHPIc neither show epigenetic nor molecular genetic changes in *GNAS*, demonstrating that PHPIc may be caused by a variety of pathogenetic mechanisms.

In summary, our molecular genetic and functional data prove impaired Gsα function by naturally occurring mutations at the Gsα encoding exons of *GNAS* as one cause of patients formerly diagnosed with PHPIc. However, since these mutations concern selectively Gsα-receptor coupling functions and show fundamental differences from those mutations associated with PHPIa, we regard this as a new subgroup of PHP. On the basis of our findings and the findings of methylation changes in patients with PHP and AHO (de Nanclares et al., 2007; Mantovani et al., 2010), a new classification of *GNAS* related disorders should be proposed in the future, based not only on clinical and laboratory alterations, but also on molecular genetic, epigenetic, and functional changes.

Acknowledgments

We thank all family members for their participation, and their physicians for sending us the samples. Moreover, we are grateful to Dagmar Struve, Christine Marschke, and Pia Staedt for excellent technical assistance. This work was supported by research grants from the German Ministry for Research and Education (BMBF No: GMG 01GM0315 to OH), a travel grant of the Fritz Thyssen Stiftung (To ST) and a research grant to LdS (Piedmont Region Funds for Finalized Research 2009, R4325). The study was furthermore supported by the Cluster of Excellence "Inflammation at interfaces" (to JG). This work was also funded, in part, by research grants from National Institute of Diabetes and Digestive and Kidney Diseases (R01DK073911 to MB and R37DK46718 to HJ).

References

Ahrens W, Hiort O, Staedt P, Kirschner T, Marschke C, Kruse K. Analysis of the GNAS1 gene in Albright's hereditary osteodystrophy. J Clin Endocrinol Metab. 2001; 86:4630–4634. [PubMed: 11600516]

Aldred MA. Genetics of pseudohypoparathyroidism types Ia and Ic. J Pediatr Endocrinol Metab. 2006; 19(2):635–640. [PubMed: 16789628]

Bastepe M, Pincus JE, Sugimoto T, Tojo K, Kanatani M, Azuma Y, Kruse K, Rosenbloom AL, Koshiyama H, Jüppner H. Positional dissociation between the genetic mutation responsible for pseudohypoparathyroidism type Ib and the associated methylation defect at exon A/B: evidence for a long-range regulatory element within the imprinted GNAS1 locus. Hum Mol Genet. 2001; 10:1231–1241. [PubMed: 11406605]

Bastepe M, Gunes Y, Perez-Villamil B, Hunzelman J, Weinstein LS, Jüppner H. Receptor-mediated adenylyl cyclase activation through XLalpha(s), the extra-large variant of the stimulatory G protein alpha-subunit. Mol Endocrinol. 2002; 16:1912–1919. [PubMed: 12145344]

Bastepe M, Jüppner H. GNAS locus and pseudohypoparathyroidism. Horm Res. 2005; 63:65–74. [PubMed: 15711092]

Bastepe M. The *GNAS* locus and pseudohypoparathyroidism. Adv Exp Med Biol. 2008; 626:27–40. [PubMed: 18372789]

De Sanctis L, Romagnolo D, Olivero M, Buzi F, Maghnie M, Soire G, Crino A, Baroncelli GI, Salerno M, Di Maio S, Cappa M, Grosso S, Rigon F, Lala R, De Sanctis C, Dianzani I. Molecular analysis of the GNAS1 gene for the correct diagnosis of Albright hereditary osteodystrophy and pseudohypoparathyroidism. Pediatr Res. 2003; 53:749–755. [PubMed: 12621129]

de Nanclares GP, Fernández-Rebollo E, Santin I, García-Cuartero B, Gaztambide S, Menéndez E, Morales MJ, Pombo M, Bilbao JR, Barros F, Zazo N, Ahrens W, Jüppner H, Hiort O, Castaño L, Bastepe M. Epigenetic defects of GNAS in patients with pseudohypoparathyroidism and mild features of Albright´s herediatary osteodystrophy. J Clin Endocrinol Metab. 2007 Jun; 92(6):2370–2373. [PubMed: 17405843]

Farfel Z, Brothers VM, Brickman AS, Conte F, Neer R, Bourne H. Pseudohypoparathyroidism: Inheritance of deficient receptor-cyclase coupling activity. Pro Natl Acad Sci. 1981; 78:3098–3102.

Hamm HE, Deretic A, Arendt A, Hargrave PA, Koenig B, Hofmann KP. Site of G protein binding to rhodopsin mapped with synthetic peptides from the alpha subunit. Science. 1998; 241:832–835. [PubMed: 3136547]

Jüppner H, Schipani E, Bastepe M, Cole DE, Lawson ML, Mannstadt M, Hendy GN, Plotkin H, Koshiyama H, Koh T, Crawford JD, Olsen BR, Vikkula M. The gene responsible for

pseudohypoparathyroidism type Ib is paternally imprinted and maps in four unrelated kindreds to chromosome 20q13.3. Proc Natl Acad Sci U S A. 1998; 95:11798–11803. [PubMed: 9751745]

Jüppner H, Linglart A, Fröhlich LF, Bastepe M. Autosomal-dominant pseudohypoparathyroidism type Ib is caused by different microdeletions within or upstream of the GNAS locus. Ann N Y Acad Sci. 2006; 1068:250–255. [PubMed: 16831926]

Kozasa T, Itoh H, Tsukamoto T, Kaziro Y. Isolation and characterization of the human Gs alpha gene. Proc Natl Acad Sci U S A. 1988; 85:2081–2085. [PubMed: 3127824]

Kraulis PJ. MOLSCRIPT: a program to produce both detailed and schematic plots of protein structures. Journal of Appl Crystallogr. 1991; 24:946–950.

Lania A, Mantovani G, Spada A. G protein mutations in endocrine diseases. Eur J Endocrinol. 2001; 145:543–559. [PubMed: 11720871]

Levine MA, Downs RW Jr, Singer M, Marx SJ, Aurbach GD, Spiegel AM. Deficient activity of guanine nucleotide regulatory protein in erythrocytes from patients with pseudohypoparathyroidism. Biochem Biophys Res Commun. 1980; 94:1319–1324. [PubMed: 6249307]

Levine MA, Ahn TG, Klupt SF, Kaufman KD, Smallwood PM, Bourne HR, Sullivan KA, Van Dop C. Genetic deficiency of the alpha subunit of the guanine nucleotide-binding protein Gs as the molecular basis for Albright hereditary osteodystrophy. Proc Natl Acad Sci U S A. 1988; 85:617–621. [PubMed: 2829196]

Linglart A, Carel JC, Garabedian M, Le T, Mallet E, Kottler ML. GNAS1 lesions in pseudohypoparathyroidism Ia and Ic: genotype phenotype relationship and evidence of the maternal transmission of the hormonal resistance. J Clin Endocrinol Metab. 2002; 87:189–197. [PubMed: 11788646]

Linglart A, Mahon MJ, Kerachian MA, Berlach DM, Hendy GN, Jüppner H, Bastepe M. Coding GNAS mutations leading to hormone resistance impair in vitro agonist- and cholera toxin-induced cAMP formation mediated by human XL{alpha}s. Endocrinology. 2006; 147(5):2253–2262. [PubMed: 16484323]

Mantovani G, Spada A. Mutations in the Gs alpha gene causing hormone resistance. Best Pract Res Clin Endocrinol Metab. 2006; 20:501–513. [PubMed: 17161328]

Mantovani G, de Sanctis L, Barbieri AM, Elli FM, Bollati V, Vaira V, Labarile P, Bondioni S, Peverelli S, Lania AG, Beck-Peccoz P, Spada A. Pseudohypoparathyroidism and GNAS epigenetic defects: clinical evaluation of Albright hereditary osteodystrophy and molecular analysis in 40 patients. J Clin Endocrinol Metab. 2010; 95(2):651–658. [PubMed: 20061437]

Masters SB, Sullivan KA, Miller RT, Beiderman B, Lopez NG, Ramachandran J, Bourne HR. Carboxyl terminal domain of Gs alpha specifies coupling of receptors to stimulation of adenylyl cyclase. Science. 1988; 241:448–451. [PubMed: 2899356]

Pantaloni C, Audigier Y. Functional domains of the Gs alpha subunit: role of the C-terminus in the receptor-dependent and receptor-independent activation. J Recept Res. 1993; 13:591–608. [PubMed: 8383762]

Rasenick MM, Watanabe M, Lazarevic MB, Hatta S, Hamm HE. Synthetic peptides as probes for G protein function. Carboxyl-terminal G alpha s peptides mimic Gs and evoke high affinity agonist binding to beta-adrenergic receptors. J Biol Chem. 1994; 269:21519–21525. [PubMed: 8063788]

Schwindinger WF, Miric A, Zimmerman D, Levine MA. A novel Gs alpha mutant in a patient with Albright hereditary osteodystrophy uncouples cell surface receptors from adenylyl cyclase. J Biol Chem. 1994; 269:25387–25391. [PubMed: 7523385]

Spiegel AM, Simonds WF, Jones TL, Goldsmith PK, Unson CG. Antibodies against synthetic peptides as probes of G protein structure and function. Soc Gen Physiol Ser. 1990; 45:185–195. [PubMed: 2116039]

Sullivan KA, Miller RT, Masters SB, Beiderman B, Heideman W, Bourne HR. Identification of receptor contact site involved in receptor-G protein coupling. Nature. 1987; 330:758–760. [PubMed: 2827032]

Sunahara RK, Tesmer JJG, Gilman AG, Sprang SR. Crystal structure of the adenylyl cyclase activator Gsα. Science. 1997; 278:1943–1947. [PubMed: 9395396]

Weinstein, LS. Albright hereditary Osteodystrophy, pseudohypoparathyroidism and Gs deficiency. In: Spiegel, AM., editor. G proteins, receptors, and desease. New Jersey: Humana Press; 1998. p. 23-56.

Weinstein LS, Chen M, Liu J. Gs(alpha) mutations and imprinting defects in human disease. Ann N Y Acad Sci. 2002; 968:173–197. [PubMed: 12119276]

Zhang L, Bastepe M, Jüppner H, Ruan KH. Characterization of the molecular mechanisms of the coupling between intracellular loops of prostacyclin receptor with the C-terminal domain of the Gαs protein in human coronary artery smooth muscle cells. Arch Biochem Biophys. 2006; 454:80–88. [PubMed: 16942748]

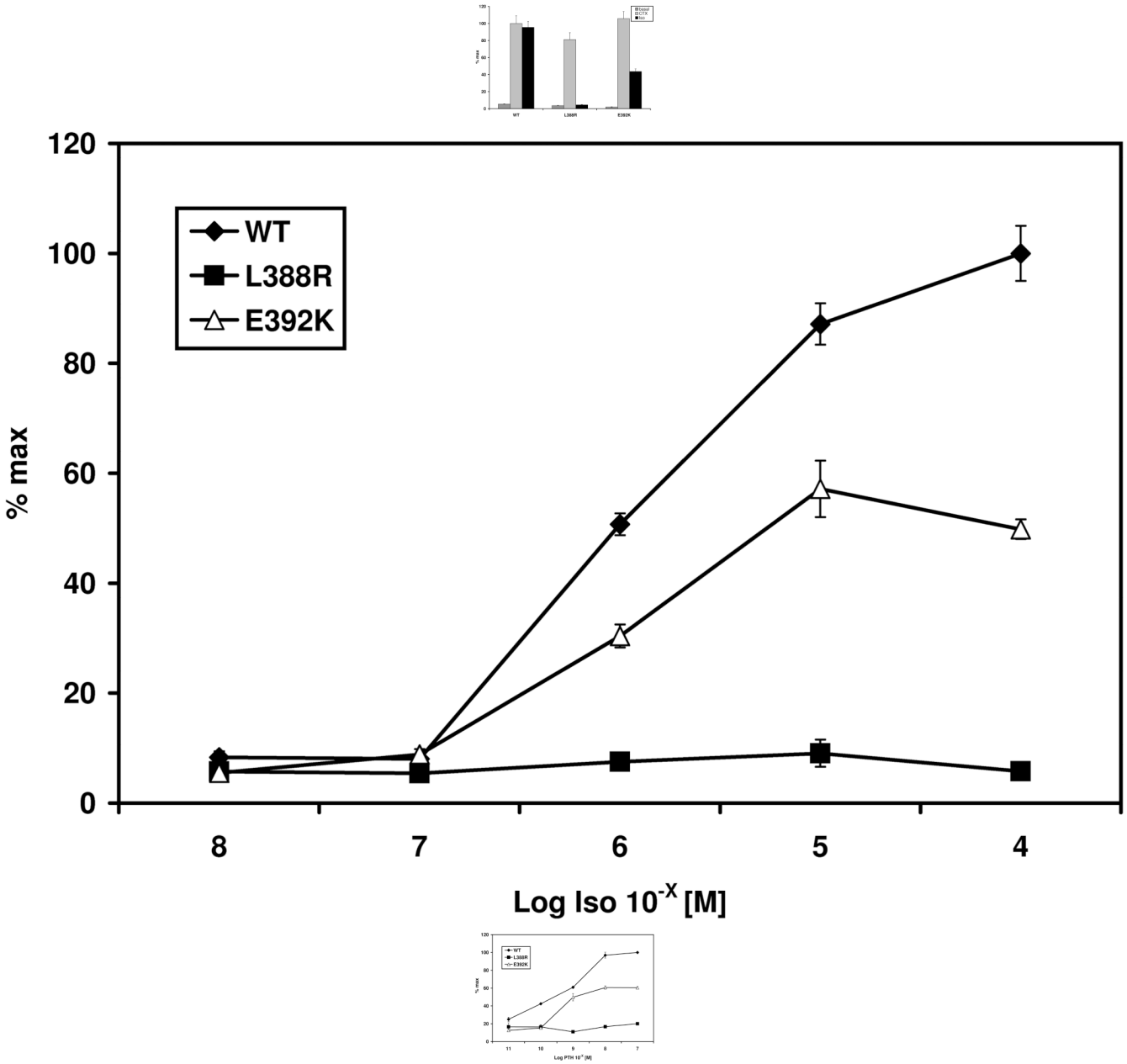

Figure 1.

Stimulation of PHPIc associated missense mutants Gsα-388R and Gsα-392K. **Panel a)** shows cAMP accumulation of both transfected missense mutants after receptor mediated stimulation of the endogenous expressed β_2-receptor due to Isoproterenol compared to receptor-independent stimulation due to CTX. The mutation p.L388R results in a loss of receptor-mediated stimulation despite normal receptor-independent activation compared to the wild-type. The Gsα-392K mutant demonstrates a diminished activity after receptor-mediated stimulation, although the receptor-independent stimulation is comparable to that of the Gsα-wild-type. % max: maximal response after stimulation of the Gsα-wild type with CTX. **Panel b)** Different concentrations of Isoproterenol (Iso) ranging from 10^{-8} to 10^{-4} M lead to a dose dependent stimulation of the β_2 receptor in the wild-type and the Gsα-392K mutant. The Gsα-388R mutant failed to induce intracellular cAMP synthesis. **Panel c)**

Similar results are shown after cotransfection with the PTHR: incubation with various concentrations of human PTH ranging from 10^{-11} to 10^{-7} M lead to a dose dependent response for the wild-type, and the Gsα-392K mutant, whereas the Gsα-388R-mutant does not show any response.

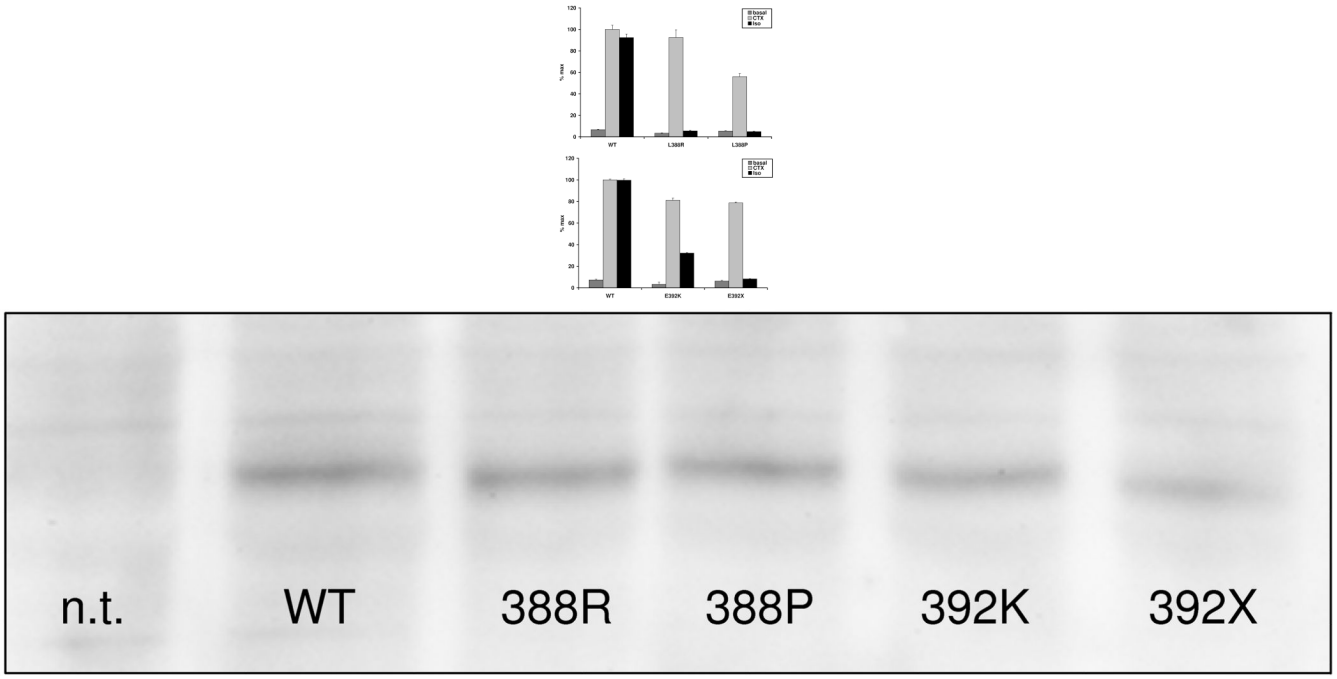

Figure 2.

PHPIc and PHPIa associated Gsα-mutants can be distinguished by in vitro stimulation tests. These experiments demonstrate that the cell model may be appropriate to reflect differences in receptor-independent activation between PHPIc and PHPIa and between the effects of missense and nonsense mutations: **Panel a)** In contrast to Gsα-388R, the Gsα-388P mutant found in a patient with PHPIa leads to a clearly diminished CTX induced cAMP synthesis that was significantly different from the corresponding cAMP levels in cells expressing Gsα-388R ($P<0.001$). **Panel b)** After receptor-mediated stimulation the Gsα-392K mutant revealed a residual activity that was absent in the nonsense mutant Gsα-392X ($P<0.001$). **Panel c)** Comparison of Gsα-protein levels in non-transfected (n.t.) and transfected $Gnas^{E2-/E2-}$ cells by immunoblot analysis. Gsα-wild-type (WT), Gsα-388R (388R), Gsα-388P (388P), Gsα-392K (392K), and Gsα-392X (392X). The protein levels of the mutants were similar to those of the wild-type.

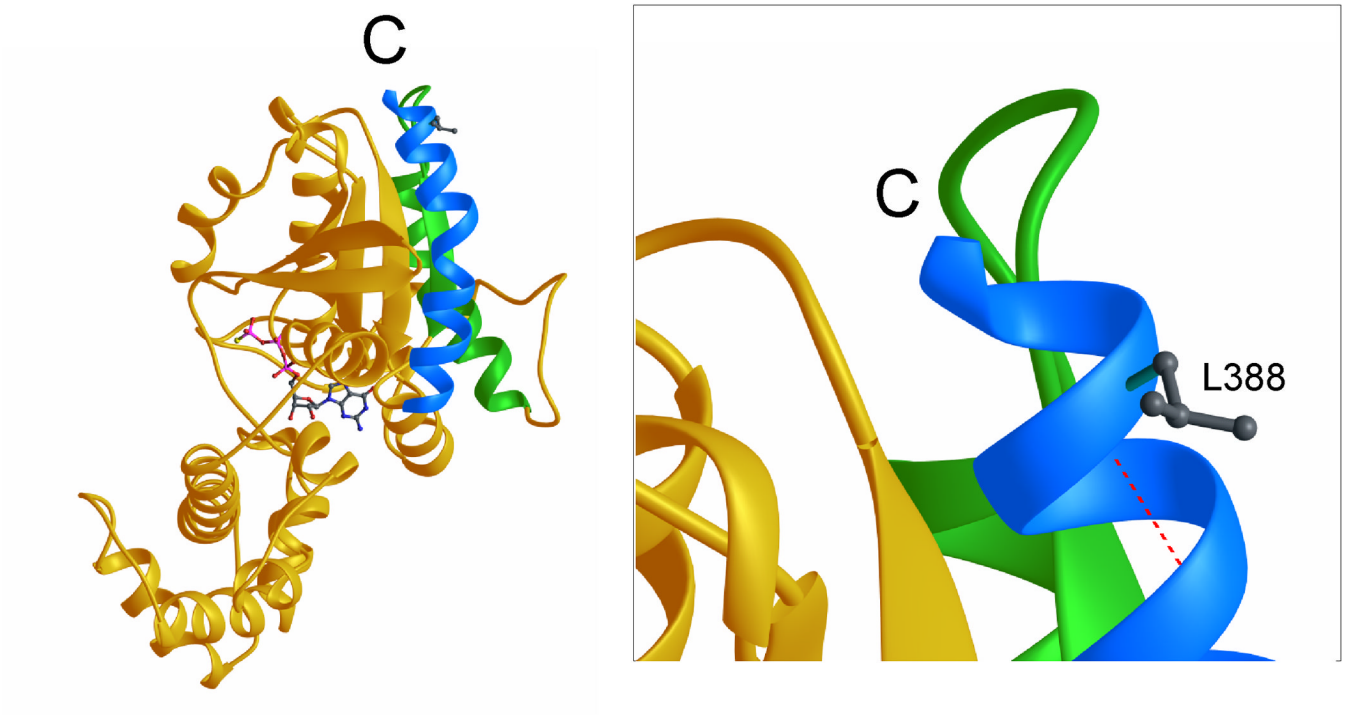

Figure 3.
Ribbon representation of Gsα in complex with GTP-γs. **Left:** The C-terminal helix (α5) is colored in light blue, the helix α4 and the β-strand β6 in green and the GTP-γs molecule is depicted as a ball and stick representation. C denotes the C-terminus. **Right:** Close-up of the C-terminal region. The side chain of L388 is depicted and the hydrogen bond between the amide group of L388 and the carbonyl group of Q384 is shown in red (dashed line).

Table 1

Subtypes of PHP and differences in phenotype, molecular genetic defects and *in-vitro* Gsα protein activity

	PHPIa	**PPHP**	**PHPIb**	**PHPIc**
AHO features	yes	yes	rarely	yes
PTH resistance	yes	no	yes	yes
***GNAS* defects**	mutations in exons 1–13	mutations in exons 1–13	epigenetic changes at the *GNAS* locus e.g. loss of methylation	not known, one mutation in exon 13 (Linglart et al., 2002)
In-vitro* Gsα protein activity	**diminished**	diminished	normal	**normal**
Transmission	maternal	paternal	maternal	maternal

The classification of PHP is based on the presence or absence of AHO features and the result of the Gsα protein activity carried out on isolated Gsα from erythrocyte membranes derived from patients. The result of the Gsα protein activity assay is the only certain difference between PHPIc and PHPIa, which is diminished in PHPIa and normal in PHPIc.

* normal range: 85–115%

Hum Mutat. Author manuscript; available in PMC 2012 June 1.

Table 2

Phenotypical, laboratory results *in-vitro* Gsα protein activity, and results of mutational analysis of our patients

Patient	**A**	**B**	**C**	**D1**	**D2**	**E**
Age at diagnosis, sex	12 years, male	5.5 years, female	11 month, female	13 years, male	13 years, female	4 years, female
Clinical features	rf, sst, bm, mr,o	rf, bm, o	rf, sst, bm	rf, bm	rf, bm, o	rf, bm, o
AHO Mother	sst, bm	bm	sst, bm	rf, sst, bm	rf, sst, bm	bm
PTH* (pg/ml; normal: 10–65)	416	133	138	643	544	286
Calcium (mmol/l; normal: 2.1–2.6)	0.84	1.1	normal	1.5	1.9	1.7
Phosphorous (mmol/l; normal: 1.09–2) age-dependent	3	2.7	2.3	3.3	2.3	3.1
TSH (mU/l; normal: 0.5–4)	9.3	6	4.7	5.9	7.4	4.5
fT3 (pg/ml; normal: 3.3–6.7)	normal	normal	normal	normal	normal	normal
fT4 (pg/ml; normal: 0.9–1.6)	normal	normal	normal	normal	normal	normal
Gsα activity in % of healthy controls (normal: 85–115)	108	102	108	100	105	71
Mutation**	c.1163T>G p.L388R	c.1174G>T p.E392X	c.1174G>A p.E392K	c.1174G>T p.E392X	c.1174G>T p.E392X	c.1163T>C p.L388P

rf: round face, sst: short stature, bm: brachymetacarpia, mr: mental retardation, o: obesity. Values in brackets define the normal range.

*all laboratory results at the time of initial diagnosis

** RefSeq: NM_000516.4

Nucleotide numbering reflects cDNA numbering system with +1 corresponding to the A of the ATG translation initiation codon in the reference sequence, according to the journal guidelines (www.hgvs.org/mutnomen).

Table 3

Sequence alignment of the α5 helix of Gsα in different species

Drosophila melanogaster	DTENIKRVFNDCRDIIQRMHLRQYELL
Xenopus laevis	DTENIRRVFNDCRDIIQRMHLRQYELL
Mus musculus	DTENIRRVFNDCRDIIQRMHLRQYELL
Macaca mulatta	DTENIRRVFNDCRDIIQRMHLRQYELL
Homo sapiens	DTENIRRVFNDCRDIIQRMHLRQYELL

The C-terminus of Gsα is highly conserved. Amino acid residues 388 and 392 are framed.